Atmospheric Environment 223 (2020) 117212

Contents lists available at ScienceDirect

Atmospheric Environment

journal homepage: http://www.elsevier.com/locate/atmosenv

Sensitivity analysis of area-wide, mobile source emission factors to high-emitter vehicles in Los Angeles

Makoto Kelp[a], Timothy Gould[b], Elena Austin[c], Julian D. Marshall[b], Michael Yost[c], Christopher Simpson[c], Timothy Larson[b,c,*]

[a] Harvard University, Department of Earth and Planetary Sciences, Cambridge, MA, 02138, USA
[b] University of Washington, Department of Civil and Environmental Engineering, Box 352700, Seattle, WA, 98195-2700, USA
[c] University of Washington, Department of Environmental and Occupational Health Sciences, Box 357234, Seattle, WA, 98195-7234, USA

HIGHLIGHTS

- Mobile monitoring sampled multi-pollutant data over urban area in-flow with traffic.
- Principal component analysis applied after *a priori* separation of high-emitters.
- Fuel-based emission factors were derived for regular heavy- and light-duty vehicles.
- We report the sensitivity of emission factors to high-emitter biasing observations.

ARTICLE INFO

Keywords:
Vehicle exhaust emission factors
High-emitting vehicles
Principal component analysis
Traffic related air pollution
Sensitivity analysis

ABSTRACT

The absolute principal component scores (APCS) model was applied to on-road, background-adjusted measurements of NO_x, CO, CO_2, black carbon (BC), and particle number (PN) obtained from a continuously moving platform deployed during 16 afternoon sampling periods in Los Angeles, CA. High-emitter biasing observations were separated from the vehicle fleet population based on a sensitivity analysis of different *a priori* screening values of the ratio of CO to CO_2. A BC/PN-rich feature consistent with heavy-duty vehicle exhaust, and a separate CO/CO_2-rich feature consistent with light-duty vehicle exhaust, described 66% of the variance of the observations. We used bootstrapped APCS model predictions to estimate area-wide, average fuel-based emission factors and their respective 95% confidence limits. If no screening was used, we obtained incongruous average emission factors relative to recent field studies for NO_x, CO, BC and PN (5.1, 2.0, 0.13 g/kg, and 1.0 × 10^15 particles/kg for heavy-duty vehicles, and 2.0, 111, 0.023 g/kg, and 0.09 × 10^15 particles/kg for light-duty vehicles, respectively). However, if reasonable *a priori* screening values were applied, which differentiate measurements reflecting high-emitter outliers, average emission factors for NO_x, CO, BC and PN (12.8, 4.0, 0.37 g/kg, and 2.6 × 10^15 particles/kg for heavy-duty vehicles, and 1.5, 40.9, 0.004 g/kg, and 0.08 × 10^15 particles/kg for light-duty vehicles, respectively) were consistent with previous estimates based on remote sensing, vehicle chase studies, and recent dynamometer tests.

1. Introduction

Research using continuously moving platforms has employed several sampling strategies to assess emissions from mobile sources in urban traffic. These mainly include "vehicle chase" studies of exhaust plumes from individual vehicles (Canagaratna et al., 2004; Durbin et al., 2008; Herndon et al., 2005; Hudda et al., 2013; Jezek et al., 2015; Jiang et al., 2005; Johnson et al., 2005; Kam et al., 2012; Kittelson et al., 2004, 2006b, 2006a; Kolb et al., 2004; Lau et al., 2015; Liggio et al., 2012; Ning et al., 2012; Park et al., 2011; Shorter et al., 2005; Westerdahl et al., 2009; Yli-Tuomi et al., 2005; Zavala et al., 2006, 2009). The impacts of vehicle emission regulations have been assessed also by combining mobile monitoring measurements with prior information on the traffic mix during sampling (Hudda et al., 2013; Johnson et al., 2009; Kozawa et al., 2014; Liggio et al., 2012).

In a previous study (Larson et al., 2017), we estimated area-wide

* Corresponding author. University of Washington, Department of Civil and Environmental Engineering, Box 352700, Seattle, WA, 98195-2700, USA.
E-mail address: tlarson@uw.edu (T. Larson).

https://doi.org/10.1016/j.atmosenv.2019.117212
Received 29 July 2019; Received in revised form 15 November 2019; Accepted 5 December 2019
Available online 9 December 2019
1352-2310/

average vehicle emission factors (EFs) for both heavy- and light-duty vehicles in Seattle by deriving absolute principal component scores (APCS) for measurements obtained from a continuously moving platform. In that study, we did not chase specific vehicles nor did we use prior traffic information to obtain both heavy- and light-duty vehicle EFs. Here we examine data obtained across a large urban area, specifically Los Angeles, CA. As in our previous study, the pollutants we measured (particle number (PN) concentration, black carbon (BC), CO, CO_2, and NO_x) were chosen based on 1) the important contribution of traffic sources to these pollutant's emissions and resulting concentrations, 2) the relative importance of these species in distinguishing emissions from light-duty versus heavy-duty vehicles (Dallmann et al., 2012, 2013; Pachon et al., 2012; Park et al., 2011), 3) the required sensitivity and response time available from "intermediate-cost" pollutant-specific monitors easily deployable on a mobile platform (Riley et al., 2014a), and 4) the recognized health effects of pollutant exposure to ultrafine particle number (Devlin et al., 2014; Peters et al., 2015), BC (Janssen et al., 2012), CO (EPA and U.S., 2010), and NO_x (EPA and U.S., 2016).

Studies suggest that high-emitter vehicles, a small, malfunctioning fraction of the vehicle fleet, can emit orders of magnitude higher emissions than regular, well-maintained vehicles, and may be responsible for a disproportionately large fraction of overall vehicle emissions (Park et al., 2011; Quiros et al., 2013; Singer and Harley, 2000; Wren et al., 2018). A case study of California vehicles noted that high-emitting vehicles might only account up to 6% of the vehicle population, yet will contribute to more than 75% of exhaust and 66% of evaporative emissions in 2030 (Collet et al., 2015). However, distinguishing between regular and high-emitting vehicles is not a concise issue. There exist multiple definitions for high-emitters that would be acceptable.

The novel contribution of this study is the presentation of a mobile monitoring framework for separating regular and high-emitting vehicles. Without this approach, estimating EFs from a mobile platform results in unrealistic and skewed EF results. This work has also the benefit of adding to the body of literature characterizing emissions from the urban vehicle fleet in Los Angeles. The results presented here can be referenced to establish threshold ranges for defining high-emitting vehicles in an urban area.

2. Material and methods

2.1. Study area

Sampling took place on 16 days during March 11–26, 2013. Sampling was divided into four routes, one on freeways and three routes on city streets (Fig. S1), with one route driven per day during 14:00–19:00 local time; the total driving time was about 80 h. The Los Angeles County road and street classifications within the sampling route (Fig. S2) and observed vehicle speed during sampling hours (Fig. S3) are included in the supplementary information. These routes were chosen in conjunction with other fixed site sampling that was a part of the MESA Air epidemiology study (Kaufman et al., 2016). As such, there was a focus on coverage of subject's at-home exposure resulting in sampling along residential streets rather than strictly freeway driving.

Emissions from Los Angeles International Airport (LAX) may impact local PN concentrations (c.f. Riley et al., 2016). As a sensitivity analysis, we reduced the potential impact of LAX emissions by excluding observations below a latitude of 34.00° (supplementary information).

2.2. Mobile monitoring measurements

The mobile monitoring platform, described previously (Riley et al., 2014b), consisted of a gasoline powered Chrysler Town & Country with two roof-mounted sampling inlets constructed of stainless steel/copper and Teflon for isokinetic sampling of particulate matter and gases, respectively.

Ten-second averages were collected simultaneously from five different instruments: Micro-Aethalometer AE52 (BC), P-Trak model 8525 with diffusion screens (PN > 50 nm), 2B Tech model 410 analyzer with model 401 converter (NO_x), Model T15x Measurer (CO), and SenseAir K-30-FS sensor (CO_2). Manufacturer, measurement range, response time for each of these instruments are provided in Table S1 (supplementary information). These devices are all moderately priced analyzers with relatively low power draw and fast enough response times to be practical and appropriate for mobile monitoring use. Sampling flow rates ranged from 0.2 L/min for the MicroAeth to 4–5 L/min for the CO and CO_2 analyzers located inside a manifold connected to an external vacuum blower downstream.

A sampling route was driven three to four times throughout the study period and a portion of the route usually repeated on a given day, such that multiple visits were made to the same locations. Routes were driven in both directions, i.e., clockwise and counter-clockwise loops, during the multiple days of coverage. The platform sampled at the speed of surrounding traffic on different types of roadways, with overall average speeds per route between 20 and 35 km/h. Variability in vehicle speed resulted in 10-s measurements spaced at variable distances from each other.

A complete description and diagram of the mobile platform is given elsewhere (Riley et al., 2014a), as well as a more complete treatment of instrument quality control objectives and evaluation methods (Larson et al., 2017). Instrument detection limits for 10-s average data are given in Table S1.

3. Theory/Calculation

3.1. Data processing and assumptions

3.1.1. Smoothing and background adjustment

The time series is smoothed each day by taking a moving block average of consecutive observations in a 70-s interval centered on a given 10-s average observation. The background concentration is computed by taking a rolling 10-min block 5th percentile value centered on the 10-s period of interest. All the smoothed, background-adjusted observations are combined, and the PCA analysis is done using all valid 10-s observation periods across all days. Rationale for these adjustments are found elsewhere (Larson et al., 2017).

3.1.2. Identification of individual exhaust plumes

The smoothed, background adjusted 10-s concentrations are further screened by removing entire samples from the initial set of observations if the background-adjusted value of CO_2 is less than 5 ppmv. This criterion is applied to more confidently ensure the presence of individual combustion exhaust plumes at concentrations above the local CO_2 background. It is less stringent than the 20 ppmv criterion previously used in many vehicle chase studies (Kam et al., 2012). Furthermore, sets of pollutant observations were removed if falling under instrument factory detection limits applicable to the 10-s data averaging time (see Table S1).

3.1.3. Removal of extreme outliers

The 99th percentile for each pollutant in the remaining data set is then computed. Ten-second samples having these high values for one or more pollutants are also removed from the data set. This criterion is necessary to remove potential skewing events (Smit and Bluett, 2011). Outliers may represent either high emission intensities from a given vehicle or relatively undiluted plumes from the same vehicle over a 10-s interval.

3.1.4. Separation of 'high-emitters'

Because we sampled across a large urban area, and therefore a large number of vehicle exhaust plumes, we screened also the observations using pre-established criteria to identify exhaust plumes from 'high-emitters'. These vehicles are a small fraction of the total vehicle population, but as a whole have a different emission distribution than the rest of the vehicle population. We separated these high-emitter data from the majority of the observations using a range of possible cutoffs values.

The remaining observations are further sorted via an *a priori* classification of high-emitters, or, "super-emitters" as coined by Park and coworkers (Park et al., 2016). They define a high-emitter as any vehicle that had an emission rate greater than 5 times the mean EFs reported from a suite of mobile monitoring campaigns in Los Angeles. Our analysis employs that same definition of high-emitters using EFs from Park et al. and other select U.S. field studies.

All sets of observations were converted into a ratio of a given pollutant over simultaneously measured CO_2 (units: grams of gaseous pollutant/kg or 10^15 particles/kg). Values above a threshold (see Table S2) were considered "high-emitters"; values below were considered "regular" vehicles. Our analysis focuses on the EFs associated with regular vehicles. Furthermore, we recognize the lack of monitoring studies that characterize high-emitting vehicles which limits the power of the Park et al. *a priori* classification criteria. Thus, we further implemented a range of thresholds spanning the top 25% of these pollutant ratios as a sensitivity analysis to the effect of specific cutoffs on the derived EFs.

To examine whether the final results were biased due to the removal of extreme outliers prior to identification of high-emitters, we also changed the order of the screening procedures. After identification of the exhaust plumes, we separated the high-emitters from the regular emitters using the criteria described in Table S2. We then applied the 99th percentile screen independently to each of the two data sets.

3.2. Absolute principal component score (APCS) model

The APCS model described by Thurston and Spengler (1985) was used for this work. Principal components analysis is first applied to the standardized, adjusted concentrations for the m-species across all days, specifically

$$Z_{i,k} = \frac{C_{i,k}^{adj} - \overline{C}_i^{adj}}{\sigma_i}(i = 1, \ldots m; k = 1, \ldots N) \tag{1}$$

where $C_{i,k}^{adj}$ has mean C_i^{adj} and standard deviation σ_i. Standardized concentrations were used rather than raw, adjusted concentrations in order to more equally weight each species in the final solution. We retain p (p $\leq$ m) principal components based on eigenvalues $>$ 0.9 and apply a Varimax rotation to these components. APCS for the Varimax rotated components are calculated from the scores, $S_{j,k}$, for the kth observation of the jth component as follows:

$$ACPS_{j,k} = S_{j,k} - (S_0)_j (j = 1, \ldots p) \tag{2}$$

where $S_{j,k}$ are the scores derived from the $Z_{i,k}$ and $(S_0)_j$ is the predicted value of the zero vector using the rotated PCA model. The $ACPS_{j,k}$ are then regressed against the $C_{i,k}^{adj}$.

$$C_{i,k}^{adj} = (b_0)_i + \sum_{j=1}^{p} b_{i,j}(ACPS_{j,k}) + \varepsilon_{i,k} \tag{3}$$

The intercept in Equation (3) is the contribution to the adjusted values from sources unaccounted for in the PCA. The predicted concentration of pollutant i ($\widehat{Y}_i$) contributed by feature j to the kth sample is then defined by Equation (4).

$$\widehat{Y}_{i,j,k} = b_{i,j}(ACPS_{j,k}) \tag{4}$$

For greater detail on rationale regarding model selection refer to Larson et al. (2017).

3.3. Fuel-based emission factors

Emission factors were reported as grams of pollutant per unit kilogram of fuel burned (g/kg):

$$EF_{i,j} = \frac{\alpha(W_c)_j}{N} \sum_{k=1}^{N} \left\{ \frac{\widehat{y}_{i,j,k}}{(\widehat{y}_{CO2})_{j,k} + (\widehat{y}_{CO})_{j,k}} \right\} \tag{5}$$

where $EF_{i,j}$ is the average fuel-based EF in grams of pollutant i per kg of fuel burned for feature j; N is the total number of samples, $(W_c)_j$ is the carbon weight fraction of the fuel corresponding to the jth feature and α is a unit conversion factor (1 μg/m^3 for CO, BC, and NO_x and 10^{12} number/cm^3 for PN).

A blocked bootstrap was applied to the above model (Equations (1)–(5)) to estimate the uncertainties in the average EFs. The blocked bootstrap was chosen to minimize potential autocorrelations owing to correlated background values not accounted for in our APCS model. We randomly sampled with replacement from non-overlapping blocks with optimal univariate block sizes determined using the "b.star" function within the "np" package in R. The maximum of the set of five univariate block sizes, corresponding to each of the five pollutant species, was chosen for bootstrap sampling. The bootstrap routine was repeated 10,000 times and 95% confidence limits were determined from the distribution of average EFs estimated from each of the 10,000 bootstrap iterations.

4. Results

4.1. Observed and background-adjusted concentrations

As described above, screened, background-adjusted observations were categorized as regular or high-emitter by applying threshold cutoffs according to Table S2. Only the CO/CO_2 ratio cutoff (164 g/kg) was applicable to this analysis as all other pollutants were below their respective species cutoff values. This CO filtering corresponded to the 91.1 percentile of this data set for Los Angeles. As such, a sensitivity analysis of percentile cutoffs was implemented only on CO/CO_2 ratios. Additional cutoff sensitivities were analyzed by removing observations spanning from the 75th to the 100th percentile [75%-85%-90%-95%-99%–100%], where the 75th percentile represents the top 25% of CO/CO_2 observations removed and the 100th percentile indicates no separation of high-emitters.

Table 1 reports the mean, median, and 95% confidence interval of the background adjusted pollutant concentrations for vehicles in Los Angeles during the field measurement campaign before CO/CO_2 cutoff values were applied.

4.2. Varimax rotated components

Varimax rotated principal component analysis of the adjusted

Table 1
Summary of background adjusted and trimmed concentrations for all measurements in Los Angeles prior to high-emitter separation (n = 11,785).

	Concentrations
PN median (mean) [#/cm^3]	5365 (7911)
PN 95% CI [#/cm^3]	1020–24827
NO_x median (mean) [ppb]	27.8 (34.0)
NO_x 95% CI [ppb]	6.1–86.8
BC median (mean), [ng/m^3]	412 (824)
BC 95% CI [ng/m^3]	120–3184
CO median (mean) [ppm]	0.46 (0.69)
CO 95% CI [ppm]	0.09–2.27
CO_2 median (mean) [ppm]	33.9 (40.6)
CO_2 95% CI [ppm]	7.7–95.7

concentration data for regular vehicles after the 91.1% cutoff for CO/CO_2 was applied resulted in two features as shown in Table 2. The Varimax rotated factor loadings and initial eigenvalues are also reported. The two component features correspond to a “BC-rich” (BC and PN) first feature and a “CO-rich” (CO and CO_2) second feature as also reported in Larson et al. (2017). Loadings and PCA results for all other percent cutoffs are found in Table S3, yielding similar findings.

4.3. Estimated fuel-based emission factors

Table 3 contains average fuel-based EFs reported by recent U.S. field studies for comparison.

Fig. 1 compares estimated average fuel-based EFs for regular-emitting vehicles in Los Angeles based on Equation (5) using CO/CO_2 ratio cutoffs spanning from removing the top 25% (75% bar in figure) to not removing any high-emitters (100% bar in figure). The blocked grey area in Fig. 1 corresponds to the approximate literature range for the given species based on Table 3, if an observation falls outside of this range then it statistically significantly exceeds those found in recent US field studies. Table S4 reports summary statistics, 95% confidence intervals and optimal univariate block sizes reflected in Fig. 1.

We notice that if the Park et al. high-emitter criteria were applied only (91.1% bar in Fig. 1), the calculated CO light-duty EF we report would exceed all those found in Table 3. By estimating CO EFs based on multiple threshold values we are able to reveal that a cutoff between 85% and 90% would offer a more favorable comparison to the suite of recent US field studies. We also notice that NO_x and PN EFs for light-duty vehicles and BC, PN, and CO EFs for heavy-duty vehicles are fairly robust against differing cutoff values as these results agree with findings from other works regardless of threshold. However, CO for light-duty vehicles and NO_x for heavy-duty vehicles become inconsistent with US field studies when a cutoff value higher than 95% of the CO/CO_2 ratio is applied. Furthermore, heavy-duty CO EFs exhibited a non-monotonic decrease as the high-emitter threshold increased. This incongruous CO behavior may be explained by recent studies of heavy-duty vehicles emitting higher CO concentrations at lower driving speeds (Grigoratos et al., 2019; Quiros et al., 2016).

There exist few studies observing EFs of high-emitting anomalies. We separate out these observations and have not reported them as they exceed the scope of this work. For illustrative purposes, EF results that do not take into account a high-emitter screening are reported in Table S4 (100% cutoff), yielding median CO EFs of 111 g/kg, statistically significantly larger than those reported for light-duty vehicles in Los Angeles in the current literature. The location of the high-emitter peaks observed during sampling as defined by the 90th percentile cutoff value (Fig. S4) was more prevalent in the low-income areas of Los Angeles consistent with the findings of Park et al. (2016).

EF results of our analysis excluding LAX for a subset of CO/CO_2 cutoffs (Table S5) were not statistically significantly different than those reported in Table S4.

4.4. Ordering of screening procedure

A screening procedure was employed based on, sequentially, 1) removal of samples with one or more pollutant concentrations above their 99th daily percentile value, 2) removal of pollutant concentrations based on the high-emitter pollutant ratio criteria found in Tables S2 and 3) applying threshold ranges of CO/CO_2 to measure the sensitivity of EFs with respect to user selected cutoffs. We also applied these screening criteria in the reverse order, i.e. 1) the high-emitter criteria found in Tables S2 and 2) the pollutant concentration above the 99th daily percentile value for a given pollutant. This consistency implies that the results here (the statistical distribution of concentrations, the APCS results, and the accompanying EFs) are not highly sensitive to the order of screening (99% trim vs. high-emitter criteria). That is, our high-emitter EF results are not biased by removing observations that include the upper 99th percentile of each species (Fig. S5).

Table 2
Varimax-rotated principal component loadings based on adjusted background concentrations for regular vehicles after the 91.1% cutoff was applied.

	PN	NO_x	BC	CO	CO_2	Initial Eigenvalue
Heavy Duty	0.81	0.64	0.87	0.01	0.14	2.10
Light Duty	0.12	0.39	−0.04	0.82	0.72	1.11

5. Discussion

We have developed a sensitivity analysis framework to separate high-emitter vehicles from the vehicle fleet population using a range of *a priori* screening values, which otherwise would result in unrealistic EF results. A multivariate analysis of air pollution from a continuously moving mobile platform was used to estimate fuel-based EFs from motor vehicles in Los Angeles, CA. Our aim was to capture the variability across a broad set of driving conditions and vehicle populations without imposing post-hoc on-road traffic or fuel-use data and without conducting specific vehicle chase studies. Our implementation of threshold cutoff criteria allowed us to remove the effect of large biasing observations using an ensemble of recent high-emitter vehicle studies. Furthermore, unlike Larson et al. (2017), this method of analysis is conducted across a large urban area as opposed to a small industrial valley in Seattle, WA. The results from this work confirm the methods and findings in Larson et al. (2017) and Wen et al. (2019) in estimating area-wide average EFs.

PCA results in Table 2 confirm a two-feature model of a heavy-duty BC- and PN-rich first feature and a light-duty CO- and CO_2-rich second feature after screening for high-emitter observations. Final results were robust against the ordering of CO/CO_2 ratio and 99th percentile trim procedures (Fig. S5). By applying a range of cutoff values when estimating area-wide EFs, we were able to attain results that agreed with both heavy- and light-duty EFs reported elsewhere (Larson et al., 2017) and in recent field studies summarized in Table 3. If only the Park et al. (2016) ‘super-emitter’ criteria were applied to our dataset (91.1% for CO/CO_2), we would still report CO light-duty EFs statistically significantly higher than literature values. However, with a range of thresholds applied, we identified a cutoff between 85 and 90% would compare favorably to literature precedent for all pollutants. We can conclude therefore that the Park et al. criteria provides a valuable framework for an *a priori* identification of high-emitting pollutants, but greater speciation of cutoffs is required for a more robust analysis.

Smoothing the 10-s observations over a 1-min period means that vehicle exhaust events (identified by increased CO_2 above background) can be due either to a single vehicle or a mix of vehicles. The average EFs can be decomposed from these mixed plumes as long as high-emitters are separated. Otherwise, these high-emitters can skew the derived factors outside of current literature precedent (100% cutoff in Table S4). The high-emitter events can be either from a single high-emitter vehicle or from a mix of both high and regular emitting vehicles. Our results indicate that high-emitter plumes, as we defined them, contain a feature that is enriched in CO relative to the regular light-duty vehicle feature, consistent with the Park et al. (2016) EFs in Table S2. In addition, the field campaign in this work took place in moderately warm temperature conditions (15–24 °C) and may be susceptible to an artificially low PN EF due to exclusion of volatile particles from our measurements, as suggested by Wang et. al. (2017).

To be sure, distinguishing between regular fleet and high-emitting vehicles is not a simple task. There exist multiple acceptable definitions for high-emitters. Therefore, this work presents an approach of implementing multiple values for such a threshold and observing how changes in that input impacts the EF results. What we have shown via a sensitivity analysis is more robust than selecting a single value for the threshold and providing only those results. However, this framework

Table 3
Derived fuel-based emission factors of recent U.S. field studies[a].

Study	Year	Sampling Type	Location	NO_x (g/kg)	CO (g/kg)	BC (g/kg)	PN (10^15/kg)
Light Duty							
This work at 85% cutoff[b]	2013	Moving in traffic	Los Angeles	1.3 [1.2–1.5]	32.7 [30.3–35.4]	0.002 [0.0006–0.004]	0.07 [0.06–0.09]
(Bishop and Stedman 2014)	2013	Roadway beam	West Los Angeles		16.4 [0.6]		
(Larson et al., 2017)	2012	Moving in traffic	Seattle	3.2 [2.8–3.6]	22.4 [19.7–25.0]	0.016 [0.011–0.021]	0.19 [0.13–0.25]
(Hudda et al., 2013)	2011	Moving in traffic	Los Angeles	3.8<1.4>		0.07<0.05>	0.43<0.26>
(Kozawa et al., 2014)	2009–2011	Moving in traffic	Los Angeles	2.7<0.4> [c], 4.0<0.3>	24<1.6>, 27<3.1>	0.015<0.011>, 0.067<0.031>	0.28<0.31>, 0.58<0.30>
(Dallmann et al., 2013)	2010	Fixed site in tunnel	Caldecott	1.90 [1.82–1.98]	14.3 [13.6–15.0]	0.010 [0.008–0.012]	
(Haugen et al., 2018b)	2017	Tent	Anaheim CA	14.5 (0.9)[d]	11.0 (2.4)		
Heavy Duty							
This work at 85% cutoff[b]	2013	Moving in traffic	Los Angeles	16.4 [12.2–23.1]	14.4 [3.1–32.4]	0.480 [0.360–0.680]	3.34 [2.5–4.8]
(Preble et al., 2018)	2014	Tunnel	Caldecott			0.41 [0.35–0.47]	
(Preble et al., 2018)	2013	Tent	Port of Oakland			0.28 [0.23–0.33]	
(Haugen and Bishop, 2017)	2015	Tent	Port of Los Angeles			0.08 (0.01)	
(Haugen and Bishop, 2017)	2015	Tent	Northern CA weight station			0.08 (0.01)	0.28 (0.0028)
(Haugen and Bishop, 2018a)	2017	Tent	Port of Los Angeles	14.6 (0.2)	1.7 (0.3)	0.03 (0.01)	1.7 (0.0014)
(Haugen and Bishop, 2018a)	2017	Tent	Northern CA weight station	9.6 (0.7)		0.06 (0.003)	0.22 (0.0026)
(Haugen and Bishop, 2018b)	2017	Tent	Anaheim CA	12.4 (0.6)	5.9 (0.9)		0.77 (0.0095)
(Larson et al., 2017)	2012	Moving in traffic	Seattle	14.8 [9.9–21.9]	18.9[8.0–35.3]	0.40 [0.29–0.58]	4.3 [2.9–6.2]
(Bishop et al., (2015)	2013	Remote sensing across road	Port of Los Angeles, Northern CA weight Station	20.7 [e] [19.1–22.3], 20.3 [18.9–22.1]	2.3 [1.5–3.1], 5.1 [4.7–5.5]	0.02 [0.014–0.026], 0.23 [0.17–0.29]	
(Preble et al., 2015)	2013	Fixed site near road	Port of Oakland	15.4 [14.5–16.3]		0.28 [0.23–0.33]	2.5 [2.0–3.0]
(Hudda et al., 2013)	2011	Moving in traffic	Los Angeles	15 <9.2>, 16 <10> [f]		0.41<0.21>, 1.33<0.33>	4.2<3.4>, 5.2<3.1>

[a] [ ] = 5th-95th percent confidence limits, < > = reported standard deviation, () = standard error.
[b] Full cutoff results for this work can be found in Table S4.
[c] Lowest and highest mean values and their corresponding standard deviations for multiple campaigns.
[d] Measurements for medium-duty vehicles.
[e] Values for separate measurements at the Port of Los Angeles and at a Northern California I-5 weigh station.
[f] Separate values for I-710 vs. other freeways.

means that we provide a range of values as the possible "answer". Though one may expect a single-value result, a multi-answer conclusion can allow for a range of potential high-emitter definitions and their sensitivities while also taking into account the historical literature of the area of analysis.

Mobile monitoring is becoming an increasingly utilized option for better understanding micro-scale differences in community level air pollution exposures. This study suggests that in addition to better characterizing community exposures, mobile monitoring also allows for researchers to estimate EFs for different localities and circumstances. Importantly, we have proposed a methodical and unique procedure to separate out skewing vehicle observations not previously addressed in the literature. Quantifying these high-emitter vehicle EFs is an area of future study that will yield a more comprehensive reflection of region-wide vehicle emission distributions. Without this approach, these observations would generally be discarded as anomalous outliers providing an incomplete estimation of emissions. The approach of Wen et al. (2019) using a combination of random spatial sampling combined with vehicle chase data is one promising approach.

For practitioners and policymakers, we demonstrate the flexibility and potential cost benefit of the APCS method that takes input information from ambient driving conditions. That is, we are able to calculate vehicle EFs and characterize the traffic mix of a city without expending resources to chase specific, individual vehicles. Furthermore, with enough spatial coverage, a spatial map of EF features may be created simply under these ambient mobile monitoring scenarios. This approach also provides information on the prevalence and location of these high-emitting vehicles and supports the previous conclusions of Park et al. (2016) that the high-emitting vehicles we identified are more prevalent in the lower income areas of Los Angeles (Fig. S4). A recent analysis by Nguyen and Marshall (2018) (Nguyen and Marshall, 2018) has independently shown that emissions near downtown Los Angeles have large impacts in terms of air pollution intake fraction, environmental justice and environmental equity. They propose a "low emission zone" that aligns with the location of many of the high-emitting vehicles we have identified. Finally, we have also shown that this method scales from a small homogeneous sampling route, located in a single industrial urban location (Larson et al., 2017) to large urban airsheds traversing multiple land use types, as demonstrated in this work.

In summary, we have formulated a methodology of applying an *a priori* classification of high-emitter vehicles to an APCS receptor model of on-road measurements of air pollution in Los Angeles, CA. In a context in which oftentimes high-emitter vehicles skew APCS (and subsequent EF) results, a suite of recent high-emitter vehicle studies was employed to establish a CO to CO_2 ratio cutoff separating regular and high-emitting vehicles. Our estimates are in agreement with these recent studies that use a variety of methods including stationary remote sensing, vehicle chase platforms, and continuously moving mobile platforms. Using the screening criteria of Park et al. (2016) to identify species exceeding high emissions and our own range of cutoff values, we were able to separate out the contribution of high-emitter vehicles that may artificially skew EF estimates using this approach (c.f. 100% cutoff

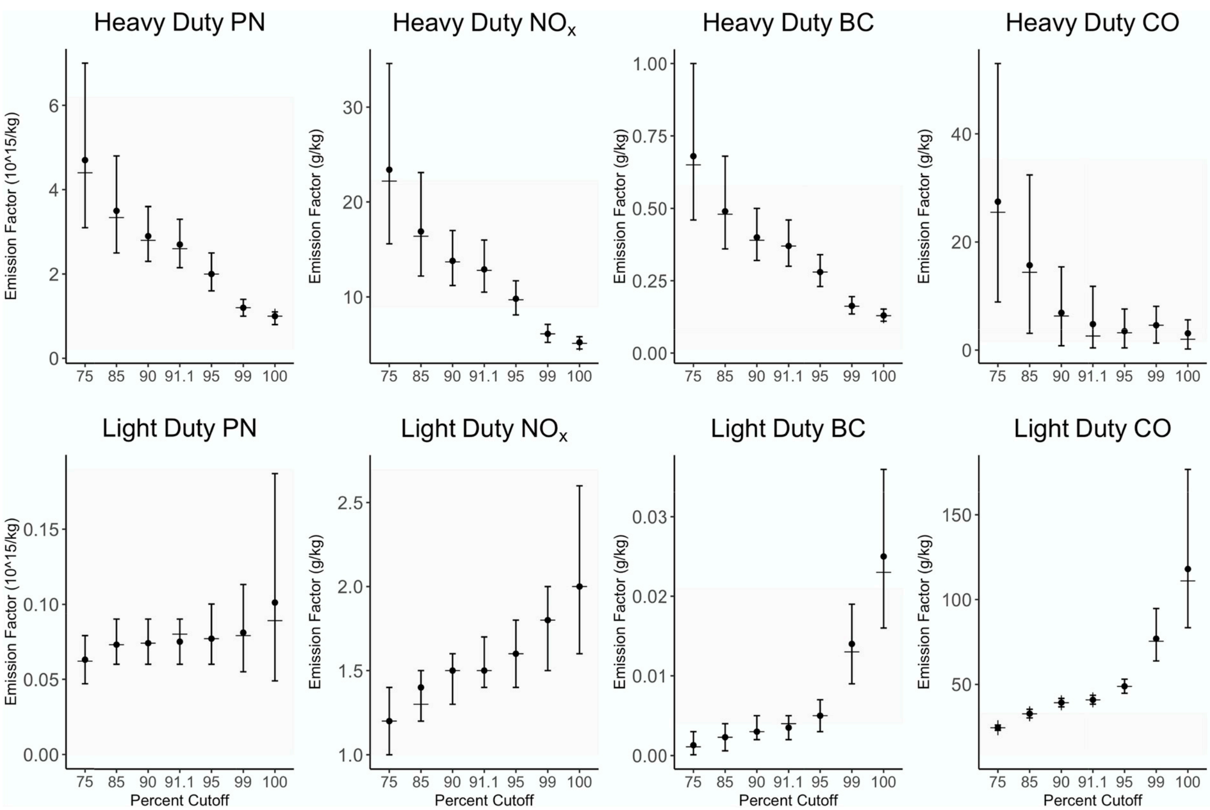

Fig. 1. Estimated fuel-based emission factors for regular-emitting vehicles determined by CO/CO_2 percentile (x axis). The error bars represent the bounds of the 95% confidence interval and the dot represents the mean of the bootstrapped distribution. The grey blocked area illustrates representative literature ranges of average EFs based on recent US field studies reflected in Table 3.

in Table S4). Our use of a multivariate model, traditionally applied for source apportionment, allows separate estimates of both heavy-duty and light-duty vehicle EFs based solely on the observed concentrations without reliance on independent traffic information.

Author contributions

Makoto Kelp: Formal analysis, Conceptualization, Software, Writing - original draft. Timothy Gould: Investigation, Data curation, Writing - original draft. Elena Austin: Software, Formal analysis, Writing - original draft. Julian D. Marshall: Supervision, Writing - original draft. Michael Yost: Project administration, Conceptualization, Writing - original draft. Christopher Simpson: Investigation, Writing - original draft. Timothy Larson: Methodology, Conceptualization, Supervision, Writing - original draft.

Declaration of competing interest

The authors declare that they have no known competing financial interests or personal relationships that could have appeared to influence the work reported in this paper.

Acknowledgements

This publication was developed under U.S. Environmental Protection Agency grant RD 83479601-0. Additional support was provided as part of the Center for Air, Climate, and Energy Solutions (CACES), which was supported under Assistance Agreement No. R835873 awarded by the U. S. Environmental Protection Agency. It has not been formally reviewed by EPA. The views expressed in this document are solely those of authors and do not necessarily reflect those of the Agency. EPA does not endorse any products or commercial services mentioned in this publication. The authors wish to thank Kris Hartin for his contribution to field data collection and Yurika Harada for her contribution to GIS visualization.

Appendix A. Supplementary data

Supplementary data to this article can be found online at https://doi.org/10.1016/j.atmosenv.2019.117212.

References

Bishop, G., Hottor-Raguindin, R., Stedman, D., McClintock, P., Theobald, E., Johnson, J., Lee, D., Zietsman, J., Misra, C., 2015. On-road heavy-duty vehicle emissions monitoring system. Environ. Sci. Technol. 49, 1639–1645.

Bishop, G.A., Stedman, D.H., 2014. The recession of 2008 and its impact on light-duty vehicle emissions in three Western United States cities. Environ. Sci. Technol. 48, 6.

Canagaratna, M., Jayne, J., Ghertner, D., Herndon, S., Shi, Q., Jimenez, J., Silva, P., Williams, P., Lanni, T., Drewnick, F., Demerjian, K., Kolb, C., Worsnop, D., 2004. Chase studies of particulate emissions from in-use New York City vehicles. Aerosol Sci. Technol. 38, 555–573.

Collet, S., Kidokoro, T., Kinugasa, Y., Karamchandani, P., DenBleyker, A., 2015. High Emitter Light Duty Vehicle Contributions to On-Road Mobile Emissions in 2018 and 2030, vol. 2, p. 7, 2015.

Dallmann, T., DeMartini, S., Kirchstetter, T., Herndon, S., Onasch, T., Wood, E., Harley, R., 2012. On-road measurement of gas and particle phase pollutant emission factors for individual heavy-duty diesel trucks. Environ. Sci. Technol. 46, 8511–8518.

Dallmann, T., Kirchstetter, T., DeMartini, S., Harley, R., 2013. Quantifying on-road emissions from gasoline-powered motor vehicles: accounting for the presence of medium- and heavy-duty diesel trucks. Environ. Sci. Technol. 47, 13873–13881.

Devlin, R., Smith, C., Schmitt, M., Rappold, A., Hinderliter, A., Graff, D., Carraway, M., 2014. Controlled exposure of humans with metabolic syndrome to concentrated ultrafine ambient particulate matter causes cardiovascular effects. Toxicol. Sci. 140, 61–72.

Durbin, T., Johnson, K., Miller, J., Maldonado, H., Chernich, D., 2008. Emissions from heavy-duty vehicles under actual on-road driving conditions. Atmos. Environ. 42, 4812–4821.

EPA, U.S., 2010. In: Assessment, N.C.f.E. (Ed.), Integrated Science Assessment for Carbon Monoxide, 2010 Final Assessment Ed. U.S. Environmental Protection Agency, Washington, DC.

EPA, U.S., 2016. Integrated science assessment for oxides of nitrogen – health criteria. In: Assessment, N.C.f.E. (Ed.), 2016 Final Report. U.S. Environmental Protection Agency, Washington, DC.

Grigoratos, T., Fontaras, G., Giechaskiel, B., Zacharof, N., 2019. Real world emissions performance of heavy-duty Euro VI diesel vehicles. Atmos. Environ. 201, 348–359.

Haugen, M., Bishop, G., 2017. Repeat Fuel Specific Emission Measurements on Two California Heavy-Duty Truck Fleets. Environ. Sci. Technol. 51, 4100–4107. https://doi.org/10.1021/acs.est.6b06172.

Haugen, M., Bishop, G., 2018a. Long-Term Fuel-Specific NO_x and Particle Emission Trends for In-Use Heavy-Duty Vehicles in California. Environ. Sci. Technol. 52, 6070–6076. https://doi.org/10.1021/acs.est.8b00621.

Haugen, M., Bishop, G., Thiruvengadam, A., Carder, D., 2018b. Evaluation of Heavy- and Medium-Duty On-Road Vehicle Emissions in California's South Coast Air Basin. Environ. Sci. Technol. 13298–13305. https://doi.org/10.1021/acs.est.8b03994.

Herndon, S., Shorter, J., Zahniser, M., Wormhoudt, J., Nelson, D., Demerjian, K., Kolb, C., 2005. Real-time measurements of SO2, H2CO, and CH4 emissions from in-use curbside passenger buses in New York City using a chase vehicle. Environ. Sci. Technol. 39, 7984–7990.

Hudda, N., Fruin, S., Delfino, R., Sioutas, C., 2013. Efficient determination of vehicle emission factors by fuel use category using on-road measurements: downward trends on Los Angeles freight corridor I-710. Atmos. Chem. Phys. 13, 347–357.

Janssen, N.A., Gerlofs-Nijland, M.E., Lanki, T., Salonen, R.O., Cassee, F., Hoek, G., Fischer, P., Brunekreef, B., Krzyzanowski, M., 2012. Health Effects of Black Carbon. World Health Organization, Copenhagen.

Jezek, I., Drinovec, L., Ferrero, L., Carriero, M., Mocnik, G., 2015. Determination of car on-road black carbon and particle number emission factors and comparison between mobile and stationary measurements. Atmos. Meas. Tech. 8, 43–55.

Jiang, M., Marr, L., Dunlea, E., Herndon, S., Jayne, J., Kolb, C., Knighton, W., Rogers, T., Zavala, M., Molina, L., Molina, M., 2005. Vehicle fleet emissions of black carbon, polycyclic aromatic hydrocarbons, and other pollutants measured by a mobile laboratory in Mexico City. Atmos. Chem. Phys. 5, 3377–3387.

Johnson, J., Kittelson, D., Watts, W., 2005. Source apportionment of diesel and spark ignition exhaust aerosol using on-road data from the Minneapolis metropolitan area. Atmos. Environ. 39, 2111–2121.

Johnson, J., Kittelson, D., Watts, W., 2009. The effect of federal fuel sulfur regulations on in-use fleets: on-road heavy-duty source apportionment. Environ. Sci. Technol. 43, 5358–5364.

Kam, W., Liacos, J., Schauer, J., Delfino, R., Sioutas, C., 2012. On-road emission factors of PM pollutants for light-duty vehicles (LDVs) based on urban street driving conditions. Atmos. Environ. 61, 378–386.

Kaufman, J.D., Adar, S.D., Barr, R.G., Budoff, M., Burke, G.L., Curl, C.L., Daviglus, M.L., Diez Roux, A.V., Gassett, A.J., Jacobs Jr., D.R., Kronmal, R., Larson, T.V., Navas-Acien, A., Olives, C., Sampson, P.D., Sheppard, L., Siscovick, D.S., Stein, J.H., Szpiro, A.A., Watson, K.E., 2016. Association between air pollution and coronary artery calcification within six metropolitan areas in the USA (the Multi-Ethnic Study of Atherosclerosis and Air Pollution): a longitudinal cohort study. Lancet 388, 696–704.

Kittelson, D., Watts, W., Johnson, J., 2004. Nanoparticle emissions on Minnesota highways. Atmos. Environ. 38, 9–19.

Kittelson, D., Watts, W., Johnson, J., 2006a. On-road and laboratory evaluation of combustion aerosols - Part 1: summary of diesel engine results. J. Aerosol Sci. 37, 913–930.

Kittelson, D., Watts, W., Johnson, J., Schauer, J., Lawson, D., 2006b. On-road and laboratory evaluation of combustion aerosols - Part 2: summary of spark ignition engine results. J. Aerosol Sci. 37, 931–949.

Kolb, C., Herndon, S., McManus, B., Shorter, J., Zahniser, M., Nelson, D., Jayne, J., Canagaratna, M., Worsnop, D., 2004. Mobile laboratory with rapid response instruments for real-time measurements of urban and regional trace gas and particulate distributions and emission source characteristics. Environ. Sci. Technol. 38, 5694–5703.

Kozawa, K., Park, S., Mara, S., Herner, J., 2014. Verifying emission reductions from heavy-duty diesel trucks operating on southern California freeways (vol 48, pg 1475, 2014). Environ. Sci. Technol. 48, 8933-8933.

Larson, T., Gould, T., Riley, E., Austin, E., Fintzi, J., Sheppard, L., Yost, M., Simpson, C., 2017. Ambient air quality measurements from a continuously moving mobile platform: estimation of area-wide, fuel-based, mobile source emission factors using absolute principal component scores. Atmos. Environ. 152, 201–211.

Lau, C., Rakowska, A., Townsend, T., Brimblecombe, P., Chan, T., Yam, Y., Mocnik, G., Ning, Z., 2015. Evaluation of diesel fleet emissions and control policies from plume chasing measurements of on-road vehicles. Atmos. Environ. 122, 171–182.

Liggio, J., Gordon, M., Smallwood, G., Li, S., Stroud, C., Staebler, R., Lu, G., Lee, P., Taylor, B., Brook, J., 2012. Are emissions of black carbon from gasoline vehicles underestimated? Insights from near and on-road measurements. Environ. Sci. Technol. 46, 4819–4828.

Nguyen, N.P., Marshall, J.D., 2018. Impact, efficiency, inequality, and injustice of urban air pollution: variability by emission location. Environ. Res. Lett. 13, 024002.

Ning, Z., Wubulihairen, M., Yang, F., 2012. PM, NOx and butane emissions from on-road vehicle fleets in Hong Kong and their implications on emission control policy. Atmos. Environ. 61, 265–274.

Pachon, J., Balachandran, S., Hu, Y., Mulholland, J., Darrow, L., Sarnat, J., Tolbert, P., Russell, A., 2012. Development of outcome-based, multipollutant mobile source indicators. J. Air Waste Manag. Assoc. 62, 431–442.

Park, S., Kozawa, K., Fruin, S., Mara, S., Hsu, Y., Jakober, C., Winer, A., Herner, J., 2011. Emission factors for high-emitting vehicles based on on-road measurements of individual vehicle exhaust with a mobile measurement platform. J. Air Waste Manag. Assoc. 61, 1046–1056.

Park, S., Vijayan, A., Mara, S., Herner, J., 2016. Investigating the real-world emission characteristics of light-duty gasoline vehicles and their relationship to local socioeconomic conditions in three communities in Los Angeles, California. J. Air Waste Manag. Assoc. 66, 1031–1044.

Peters, A., Hampel, R., Cyrys, J., Breitner, S., Geruschkat, U., Kraus, U., Zareba, W., Schneider, A., 2015. Elevated particle number concentrations induce immediate changes in heart rate variability: a panel study in individuals with impaired glucose metabolism or diabetes. Part. Fibre Toxicol. 12.

Preble, C., Cados, T., Harley, R., Kirchstetter, T., 2018. In-Use Performance and Durability of Particle Filters on Heavy-Duty Diesel Trucks. Environ. Sci. Technol. 52, 11913–11921.

Preble, C., Dallmann, T., Kreisberg, N., Hering, S., Harley, R., Kirchstetter, T., 2015. Effects of particle filters and selective catalytic reduction on heavy-duty diesel drayage truck emissions at the Port of oakland. Environ. Sci. Technol. 49, 8864–8871.

Quiros, D., Zhang, Q., Choi, W., He, M., Paulson, S., Winer, A., Wang, R., Zhu, Y., 2013. Air quality impacts of a scheduled 36-h closure of a major highway. Atmos. Environ. 67, 404–414.

Quiros, D.C., Thiruvengadam, A., Pradhan, S., Besch, M., Thiruvengadam, P., Demirgok, B., Carder, D., Oshinuga, A., Huai, T., Hu, S., 2016. Real-World emissions from modern heavy-duty diesel, natural gas, and hybrid diesel trucks operating along major California freight corridors. Emiss. Control Sci. Technol. 2, 156–172.

Riley, E., Banks, L., Fintzi, J., Gould, T., Hartin, K., Schaal, L., Davey, M., Sheppard, L., Larson, T., Yost, M., Simpson, C., 2014a. Multi-pollutant mobile platform measurements of air pollutants adjacent to a major roadway. Atmos. Environ. 98, 492–499.

Riley, E., Gould, T., Hartin, K., Fruin, S., Simpson, C., Yost, M., Larson, T., 2016. Ultrafine particle size as a tracer for aircraft turbine emissions. Atmos. Environ. 139, 20–29.

Riley, E.A., Banks, L., Fintzi, J., Gould, T.R., Hartin, K., Schaal, L., Davey, M., Sheppard, L., Larson, T., Yost, M.G., Simpson, C.D., 2014b. Multi-pollutant mobile platform measurements of air pollutants adjacent to a major roadway. Atmos. Environ. 98, 492–499.

Shorter, J., Herndon, S., Zahniser, M., Nelson, D., Wormhoudt, J., Demerjian, K., Kolb, C., 2005. Real-time measurements of nitrogen oxide emissions from in-use New York City transit buses using a chase vehicle. Environ. Sci. Technol. 39, 7991–8000.

Singer, B.C., Harley, R.A., 2000. A fuel-based inventory of motor vehicle exhaust emissions in the Los Angeles area during summer 1997. Atmos. Environ. 34, 1783–1795.

Smit, R., Bluett, J., 2011. A new method to compare vehicle emissions measured by remote sensing and laboratory testing: high-emitters and potential implications for emission inventories. Sci. Total Environ. 409, 2626–2634.

Thurston, G., Spengler, J., 1985. A quantitative assessment of source contributions to inhalable particulate matter pollution in metropolitan Boston. Atmos. Environ. 19, 9–25.

Wang, J., Jeong, C.-H., Zimmerman, N., Healy, R., Hilker, N., Evans, G., 2017. Real-World Emission of Particles from Vehicles: Volatility and the Effects of Ambient Temperature. Environ. Sci. Technol. 51, 4081–4090. https://doi.org/10.1021/acs.est.6b05328.

Wen, Y., Wang, H., Larson, T., Kelp, M., Zhang, S., Wu, Y., Marshall, J.D., 2019. On-highway vehicle emission factors, and spatial patterns, based on mobile monitoring and absolute principal component score. Sci. Total Environ. 676, 242–251.

Westerdahl, D., Wang, X., Pan, X., Zhang, K., 2009. Characterization of on-road vehicle emission factors and microenvironmental air quality in Beijing, China. Atmos. Environ. 43, 697–705.

Wren, S.N., Liggio, J., Han, Y., Hayden, K., Lu, G., Mihele, C.M., Mittermeier, R.L., Stroud, C., Wentzell, J.J.B., Brook, J.R., 2018. Elucidating real-world vehicle emission factors from mobile measurements over a large metropolitan region: a focus on isocyanic acid, hydrogen cyanide, and black carbon. Atmos. Chem. Phys. 18, 16979–17001.

Yli-Tuomi, T., Aarnio, P., Pirjola, L., Makela, T., Hillamo, R., Jantunen, M., 2005. Emissions of fine particles, NOx, and CO from on-road vehicles in Finland. Atmos. Environ. 39, 6696–6706.

Zavala, M., Herndon, S., Slott, R., Dunlea, E., Marr, L., Shorter, J., Zahniser, M., Knighton, W., Rogers, T., Kolb, C., Molina, L., Molina, M., 2006. Characterization of on-road vehicle emissions in the Mexico City Metropolitan Area using a mobile laboratory in chase and fleet average measurement modes during the MCMA-2003 field campaign. Atmos. Chem. Phys. 6, 5129–5142.

Zavala, M., Herndon, S., Wood, E., Jayne, J., Nelson, D., Trimborn, A., Dunlea, E., Knighton, W., Mendoza, A., Allen, D., Kolb, C., Molina, M., Molina, L., 2009. Comparison of emissions from on-road sources using a mobile laboratory under various driving and operational sampling modes. Atmos. Chem. Phys. 9, 1–14.